metals

MDPI

Review

Rheological Characterization of Semi-Solid Metals: A Review

Michael Modigell [1,*], Annalisa Pola [2] and Marialaura Tocci [2]

[1] Department of Engineering, German University of Technology in Oman (GUtech), PO Box 1816, Athaibah PC 130, Muscat, Oman

[2] DIMI—Mechanical and Industrial Engineering Department, University of Brescia, Via Branze, 38, 25123 Brescia, Italy; annalisa.pola@unibs.it (A.P.); marialaura.tocci@unibs.it (M.T.)

* Correspondence: michael.modigell@gutech.edu.om or michael.modigell@avt.rwth-aachen.de; Tel.: +968-2206-1110

Received: 18 February 2018; Accepted: 4 April 2018; Published: 7 April 2018

Abstract: In the present review, the main findings on the rheological characterization of semi-solid metals (SSM) are presented. Experimental results are a fundamental basis for the development of comprehensive and accurate mathematics used to design the process effectively. For this reason, the main experimental procedures for the rheological characterization of SSM are given, together with the models most widely used to fit experimental data. Subsequently, the material behavior under steady state condition is summarized. Also, non-viscous properties and transient conditions are discussed since they are especially relevant for the industrial semi-solid processing.

Keywords: rheology; semi-solid alloys; thixotropy; rheometer; compression test; viscosity

1. Introduction

In the early 1970s Flemings and coworkers [1] discovered metallic alloys in the semi-solid state with non-dendritic structure to have special rheological properties which can be exploited for a new, attractive forming process. The non-dendritic structure can be easily achieved by stirring the alloy while cooling it from the liquid state down into the semi-solid temperature range. This results in a suspension consisting of a liquid metallic phase and primary solid particles with globular or rosette-type shape [2,3], such as that shown in Figure 1, in comparison with a typical dendritic microstructure.

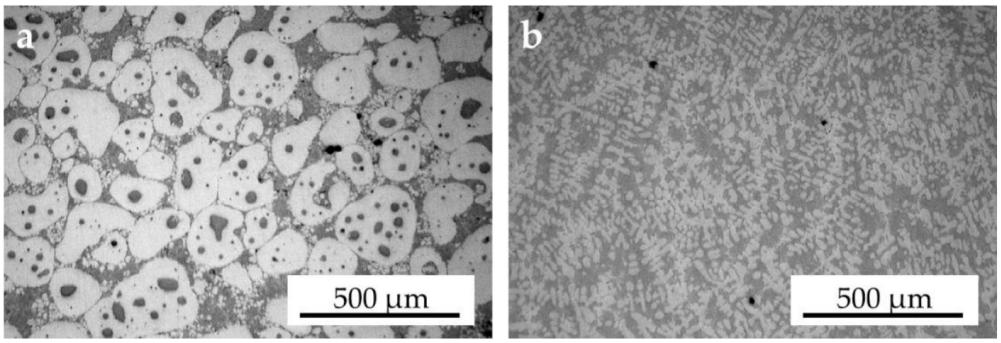

Figure 1. Typical microstructures of an A356 component obtained by (**a**) thixocasting (billet preheated to a solid fraction of 0.52–0.54) and (**b**) conventional casting (pouring temperature = 680 °C).

The rheological properties of this special type of slurry give the advantages of the semi-solid metals (SSM)-processing. In detail, the slurry can either flow like a liquid—but with non-constant

viscosity—or it can behave like a solid. This is typical for suspensions with high solid fraction (*Fs*) [4], whereas fully liquid metals show Newtonian flow behavior, which is water-like [5]. The rheological properties are responsible for the die-filling behavior of SSM, which is different from fully liquid (or fully solid) materials [6,7] and which results in specific advantages in the quality of the product (low gas porosity, less shrinking, higher mechanical properties, etc.), besides those related to technological aspects (longer tool life in comparison with conventional casting processes due to the lower metal temperature, etc.) [2]. To obtain these advantages, it is necessary to fully understand the rheology of the material. This enables understanding of flow-specific phenomena, such as instabilities or segregation, and allows optimization of the process. Carefully performed experiments with respect to the mechanical, fluid dynamical, and thermal conditions lead to the development of comprehensive and accurate mathematical models, which picture the physics properly and which are used in computer simulation to design and optimize the process effectively.

Few publications provide a comprehensive discussion on the rheological behavior of SSM [8,9]. In addition, in this regard, it should be mentioned that still some aspects about the flow of semi-solid metals are not clear or contradict data are available in the literature [8]. For this reason, it appears useful to provide an overview of the current knowledge about this topic, with particular attention to the scientific innovation that took place in the past 10–15 years, while details about semi-solid metal processing can be found elsewhere [2,7,10].

In Section 2, the rheological classification of SSM is explained. In Section 3, the principles of the most frequently used devices for investing rheological properties of SSM are presented: in Section 3.1 the rotational rheometer and in Section 3.2 the compression test. Section 4 gives a summary of the applied rheological models and the corresponding constitutive equations. An overview of recent published results of the equilibrium viscosity of Al-alloys is given in Section 5. Section 6 deals with special rheological phenomena of SSM: yield stress and thixotropy. Section 7 explains the influence of Ostwald ripening in rheological experiments, which is important to consider for long-term experiments.

Before analyzing the literature, it is useful to clarify some rheological terms that are related with the rheological properties of SSM and which are frequently used improperly in the literature of SSM processing.

2. Rheological Classification of SSM

The rheological behavior of any material is found to be between two limiting, ideal cases: the ideal solid body (Hookean body), which shows deformation proportional to the stress, and the ideal viscous material (Newtonian body), which shows rate of deformation proportional to the stress. Within the viscous materials, besides the Newtonian fluids (with constant viscosity, only depending on temperature and pressure), we find the Non-Newtonian fluids. Among these, we have the non-linear pure viscous fluids, whose viscosity depends additionally on the stress and which exhibit shear thinning or shear thickening behavior. Another class of the non-linear materials are the plastic ones, which show solid behavior below a certain threshold of stress (yield stress), while they are characterized by linear (Bingham body) or non-linear behavior above the yield stress. Another class of materials shows time-dependent properties, whose rheological properties do not change immediately after change in strain but follow a specific kinetics. Viscoelastic materials have simultaneously elastic and viscous properties. Thixotropic materials show a gradual decrease of viscosity under constant stress and a recovery of the viscosity when the stress is removed; in particular, the viscosity of the initial condition will be recovered totally. As shown in Figure 2, due to thixotropy, at the beginning of shearing or after a rapid change in shear rate, the instantaneous viscosity is different from the steady state values, and it takes time for the viscosity to reach a constant value, which reflects the equilibrium condition of the structure. The opposite behavior, an increase of viscosity with time, is called rheopexy.

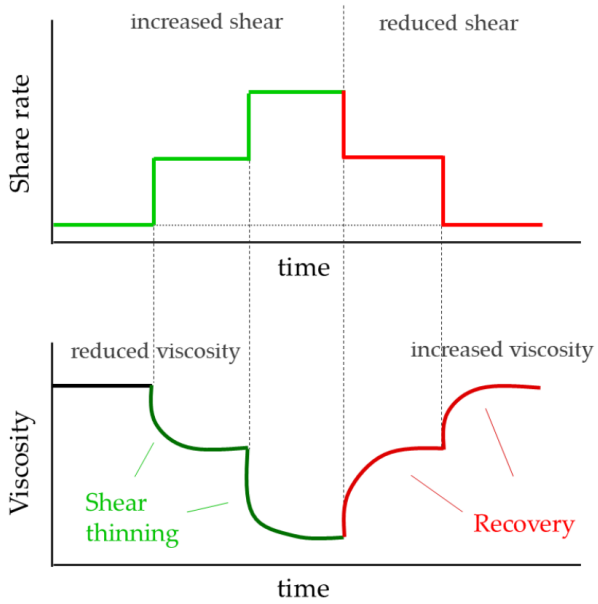

Figure 2. Schematic diagram showing the change in viscosity with time following changes in shear rate to illustrate the thixotropic behavior of semi-solid slurries [11].

Regarding the rheological classification of SSM, it is generally accepted that they are shear thinning fluids, that means that viscosity will drop with increasing shear rate (Figure 3) [12]. Additionally, they are thixotropic materials.

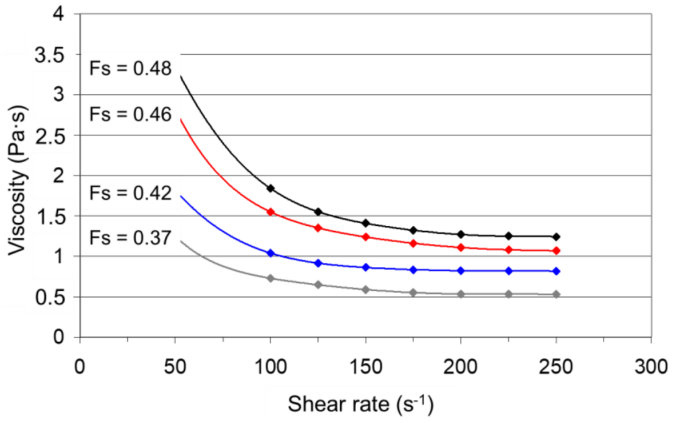

Figure 3. Example of plot of viscosity measurements in isothermal conditions from shear rate experiments for A356 alloy at various solid fractions showing the typical shear thinning behavior of SSM [12].

Finally, SSM with high solid fraction exhibit yield stress, which is nicely demonstrated with the picture of a block of Al alloy in the semi-solid state able to wear its own weight and which can be cut with an ordinary knife. A representative image of this phenomenon is shown in Figure 4; analogous pictures are available in the scientific literature, as for instance in [1].

The specific rheological properties are finally nothing more than the consequences of the changes in the internal structure of the slurry due to external forces. A simple physical model can be set up, in agreement with the general understanding of the kinematics of the SSM. It can be assumed that cohesive forces are acting between the particles of the SSM, resulting in the formation of agglomerates [13]. The particles of such agglomerates can be connected temporarily by formation of welded necks or e.g., by capillary forces. Within the agglomerates, a certain amount of liquid is

immobilized, which leads to a higher apparent solid fraction [14]. Under the influence of shear forces, the agglomerates will be partially or totally disintegrated whereby the liquid phase is released and the apparent solid fraction will approach the true fraction. With this model, the steady state behavior of the material, i.e., shear thinning, can be explained since the viscosity decreases with decreasing solid fraction.

Figure 4. Billet of a semi-solid metal cut with an ordinary knife.

By reducing the shear rate, particles that meet in the shear field have the chance to agglomerate, resulting in an increase in the apparent solid fraction.

It follows that the structural change is reversible, which explains one feature of thixotropy. The deagglomeration and agglomeration processes do not happen instantaneously, but they take some time. The agglomeration is diffusion controlled and, therefore, it is much slower than the deagglomeration phenomenon.

Similar to other suspensions, the most important parameter influencing the rheological properties is the solid fraction, which depends on the temperature [2]. Experimental measurements show that an increase in solid fraction results in an increase of viscosity. In addition, also the yield stress increases with higher solid fraction, as demonstrated in scientific literature [15–18], together with the presence of the thixotropic effects. Other factors, such as particle diameter, or diameter distribution, and the shape of the particles are of minor importance. Both these parameters can be combined with the specific surface area of solid and liquid phase. The dependency on the viscosity of the liquid phase is not very strong because the liquid phase viscosity is orders of magnitude lower than of the SSM.

This rather simple structural model has been accepted widely—although there is no clear experimental evidence. Indeed, all metallographic micrographs have been produced from ordinary solidified samples with low cooling rates. It has been demonstrated [19,20] that, with cooling rates smaller than -10 K/s, diffusional processes will significantly change the size of the particles and, therefore, the appearance of the structure. To investigate the structure is difficult. There are only a few publications [20–24] that are dealing with structural experiments with X-ray tomography for SSM in rest and compression. However, up to now, no work has been published for investigations of SSM under pure shear. The evaluation of the X-ray images shows that with increasing shear rate the distribution of the particles will become more homogenous over the volume, which confirms qualitatively the physical model [24]. The compression experiment under the X-ray beam shows that for high solid fraction (0.70) the material behaves as a saturated sponge and the liquid phase is pressed out of the skeleton with the consequence that the solid fraction will change locally. This has been previously found, as well by analyses of the solid distribution in a billet after compression [25].

3. Experimental Methods for the Measurements of Rheological Properties

3.1. Shear Experiments in Rotational Rheometers

The most widely used shear rheometers for the study of semi-solid metals are the rotational rheometers with concentric arranged cylinders. The outer cylinder is a cup that contains the SSM

material and in which the inner cylinder, the bob, is inserted. In the Couette-type rheometer the cup is rotating and the bob is fixed, whereas in the Searle rheometer the bob is rotating while the cup is fixed. Because of the relative movement of cup and bob, the material is sheared in the gap between them. The shear stress at the wall is related to the torque, which is measured, and the shear rate is related to the rotational speed and to the geometry. Due to inertia forces, the Searle system is sensitive for secondary flows, the Taylor vortices, which dissipate energy and cause an increase in the measured torque [26]. Depending on the geometry of the system and the properties of the sample, the vortices can occur already at rather low rotational speed. Simple criteria are available to calculate the onset of the vortices [26], which can be applied for all viscous fluids. Another effect that falsifies the measurements consists in turbulent vortices that occur for both rheometers at higher rotational speeds, which is defined by a critical Re number [27].

For Newtonian fluids, the evaluation of the viscosity from the torque and the rotational speed is rather simple. For non-Newtonian fluids, it is complicated when the rheological nature of the fluid is unknown. In this case, frequently the way of evaluation valid for Newtonian fluids is applied. This results in an apparent viscosity value and in an apparent flow curve, which does not reflect properly the physical properties of the material. For purely viscous materials, the approach of the representative shear location should be applied [28], which results in physical correct values. Alexandrou et al. [29] have shown recently that this method does work for viscoplastic materials in special cases only. In general, the processing of data collected from rotational rheometer should be evaluated with the help of computational rheology [30].

Wall slip is another phenomenon that affects rheological measurements in suspensions with any kind of shear device. The slip is caused by segregation of a thin layer of the liquid phase adjacent to the wall. This thin layer has the effect of a lubricant that reduces the friction and, consequently, the torque measured by rotational rheometers, resulting in apparently lower viscosity values. In the literature, some different geometries for the bob have been proposed to avoid slip. For instance, Modigell et al. [31] have shown that vane-type bobs are not suitable because they lead to secondary flows that influence torque measurements, whereas a grooved bob prevents slip without affecting the torque significantly. Another way to treat slip is to apply the Kiljanski method for Searle or Couette rheometers [32] (or the Mooney method for capillary systems). The idea of both methods is to evaluate the slip velocity with the help of two different geometries. Harboe et al. [33] could show that the application of the Kiljanski method results in the same flow curve as the application of a grooved rod, but it requires significantly more experimental effort.

For SSM with low solid fraction—and low corresponding viscosity—the influence of the surface tension on the experimental result must be considered. Tocci et al. [34] could demonstrate that small deviation of the symmetry of the measuring system leads to secondary forces caused by the surface tension, which is dominant for small shear rates. Consequently, the material appears to be strongly shear thinning, although it is almost Newtonian.

At the beginning of the development of SSM processes, most of the rheological investigations have been performed with low melting Sn-Pb alloys because of the lack of high temperature rheometers. Nowadays, commercial instruments for testing Al alloys are available, while, to our knowledge, only one commercial instrument is available on the market for studying steels [35]. Yekta et al. [36] and Modigell et al. [37] have used own developed instruments.

Typically, for experiments with rotational rheometers, a first important part of the procedure is the preparation of the semi-solid material by shearing it for a certain time during cooling to the desired temperature, according to the solid fraction. A proper material preparation is fundamental, especially under consideration of the Ostwald ripening (see Section 7), since the flow behavior of semi-solid metals is strongly related to the microstructure [2]. An example of the evolution of viscosity during the material preparation is presented in Figure 5 for an Al-Si alloy for a constant shear rate of 100 s^{-1} [12]. First, the material is sheared in the fully liquid state (630 °C) to ensure the homogeneity of the material. When the temperature decreases, a severe increase in viscosity takes place, mainly due to the formation

of solid particles. Finally, when the temperature reaches the value corresponding to the desired solid fraction (0.35 at 583 °C), a first steep decrease in viscosity is observed due to the change of dendrites into globular particles because of the application of shear forces. The following less steep decrease of the viscosity is due to Ostwald ripening.

Values of viscosity for the evaluation of flow curve in steady state condition are calculated from experimental data at different shear rates.

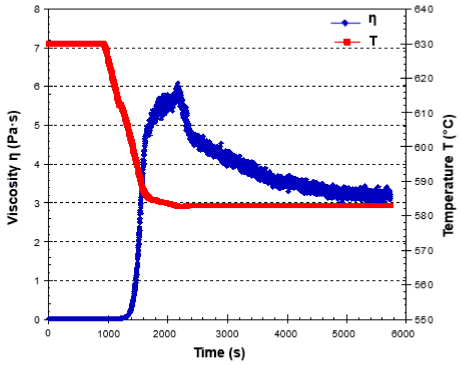

Figure 5. Plot of viscosity versus time at constant shear rate (100 s^{-1}) during cooling from liquid state (630 °C) to semi-solid condition (solid fraction of 0.35 at 583 °C) for an Al-Si alloy measured by means of a Searle rheometer [12].

3.2. Compression Tests

The compression test is a conventional testing method to acquire strain-stress curves by squeezing a sample either under a constant load between two parallel plates or with a constant speed of displacement of the plates [38]. Compression experiments are usually performed with materials characterized by a solid fraction higher than 0.5.

Various experimental configurations are possible according to the used device, an example is shown in Figure 6. Usually, the sample is first heated to the required temperature in a separate furnace or directly in the testing chamber, while, after compression, it can be quenched in water for further study of the microstructure. The applied force and the obtained displacement is monitored by a proper load cell.

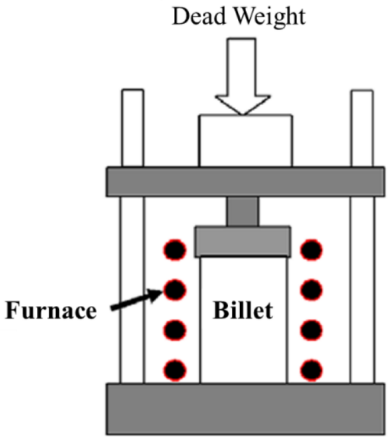

Figure 6. Scheme of parallel plate deformation set up [39].

From the stress-strain curve, it is possible to calculate rheological parameters and obtain a flow curve in terms of viscosity as a function of the shear rate, as illustrated by Laxmanan et al. [40]. It is important to mention that, with this method, the viscosity at a given shear rate is calculated under the assumption of Newtonian behavior (comparable to the simple approach with rotational rheometers).

Consequently, the calculated viscosities are apparent values only. Nevertheless, the evidence of the shear thinning behavior of SSM is obtained when the values of apparent viscosity calculated at different shear rates are compared.

Another drawback is the flow condition at the surfaces of the plates. For pure shear flow, the material should adhere to the plates. Slipping conditions result in elongation flow, which must be evaluated in a different way. In practice, none of the two conditions are completely fulfilled and the flow is of mixed mode. Additionally, the flow is non-stationary and at least 2-dimensional. Since usually the ram speed is high in order to simulate forging conditions, high accelerations are achieved, and the evaluation of thixotropic effects is difficult (as it is discussed in Section 6). At this regard, Hu et al. [40] performed compression tests with Al alloy under conditions close to forging processes and applied ram speeds up to 1000 mm/s, which results in experimental times of approximately 0.01 s. Similar values were achieved by Becker et al. [41,42] during experiments with steel.

Two practical problems arise with SSM during compression. Even at low ram speeds liquid phase is squeezed out of the sample when solid fraction is less than 0.80. This results in an inhomogeneous composition of the sample, which additionally is changing by time, although the experiments have been performed isothermally. Moreover, another problem is the cracking of the free surface with increasing deformation [43].

Temperature and compression rate can be varied to reproduce real cavity die-filling conditions, which is one advantage of this technique in comparison with shear experiments. On the other hand, the possible experimental procedures are wider for shear experiments, allowing to completely characterize the rheological behavior of the material.

Particularly, the compression rate is a key parameter since a slow compression can provide information not adequate for the understanding of the actual industrial process, which is known to take place in less than 1 s. For this reason, rapid compression tests were carried out to investigate the transient behavior of SSM [44–46]. A schematic representation of the load-displacement curve for these kinds of experiments is shown in Figure 7.

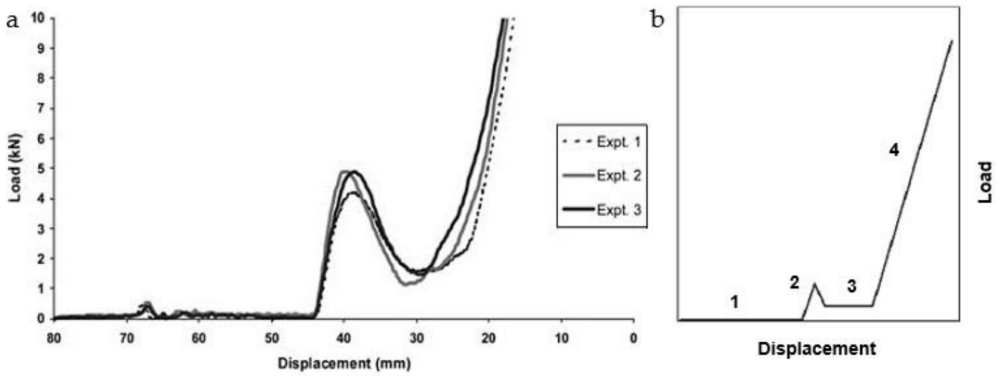

Figure 7. (**a**) Typical signal response to rapid compression of semi-solid A356 alloy (ram speed: 500 mm/s; soak time: 0 min; and temperature 575 °C) [44]; (**b**) Schematic appearance of a load vs. displacement response. Four distinct regions are present: (1) zero load prior to reaching the die; (2) an initial breakdown, or peak load (stress); (3) a relatively constant, or plateau, load after the initial breakdown; and (4) a rapid increase in the load as the die approaches complete filling [45].

In addition, the test temperature and the holding time in isothermal condition should be carefully chosen when the main aim of the experiments is to provide information adequate for the industrial process.

Finally, this experimental procedure can be applied using a close die to investigate the liquid flow during compression. This is helpful in predicting the formation of liquid segregation and surface cracks

in the products obtained by SSM processing [47]. Also, drained compression tests can be performed to investigate the compressibility of the solid phase in isothermal condition [10].

4. Modelling of Rheological Properties

The evaluation of experimental rheological investigations should result in mathematical equations, called constitutive models, which should reflect the physics of the flow and the deformation process. Surely, it is difficult to include all phenomena in one model and it is generally accepted to make simplifications according to the application of the model. The simplest models are the one phase, equilibrium models, which assume the SSM to be a homogenous fluid without time-dependent properties. Under these assumptions, the Ostwald-de-Waele model—or power law—is the simplest one, assuming viscous properties only. The relationship between shear stress and shear rate can be expressed by the following equation:

$$\tau = m\,\dot{\gamma}^{n} \tag{1}$$

And the apparent viscosity is given by:

$$\eta = \tau/\dot{\gamma} = m\,\dot{\gamma}^{n-1} \tag{2}$$

where for $n < 1$, the fluid exhibits shear thinning properties; $n = 1$, the fluid shows Newtonian behavior; $n > 1$, the fluid shows shear-thickening behavior.

The terms m and n are two empirical parameters, the flow index and shear exponent, respectively.

Because of the simplicity of this equation, it is widely applied to process data from rheological experiments. Besides the first studies on the characterization of the rheological behavior of semi-solid slurries [38,48], mainly focused on SnPb15 alloy, also more recent papers used the Ostwald-de-Waele relationship to express the viscosity as a function of shear rate for various Al alloys and steels [49,50].

The simplicity relates to a couple of disadvantages. First, the flow index m does not have a fixed dimension because this depends on the power index. More serious is the fact that for small and large shear rates the equation results in physically non-correct values. This gives problems in its application in numerical simulation. Frequently Ostwald de Waele parameters are presented with shear exponents less than zero. This will result in physically nonsensical results, as e.g., a positive pressure gradient in a simple tube flow.

The Herschel-Bulkley equation is typically used to describe the flow of viscoplastic fluids [26]. It is a generalization of the Bingham plastic model to consider the case of a non-linear relationship between shear stress and shear rate [51].

$$\tau = \tau_y + \; m\,\dot{\gamma}^{n} \tag{3}$$

With τ_y the yield stress and m and n the flow index and the shear exponent.

It is believed τ_y to be a fundamental parameter for the modeling of semi-solid metals behavior [52]. For this reason, a Herschel-Bulkley model was applied to the numerical simulation of the semi-solid processing [30,53,54], fitting experimental results for Sn-Pb15 alloy. More recently, the same model was modified to better describe the phenomena taking place in the early stages of deformation of the solid structure [30].

To model thixotropy, three main approaches are applied. One is to describe the change in the structure with the change of the viscosity, which needs to define a rate equation for the temporal development of the viscosity [55]. Another approach is to calculate the number of existing and broken connections between the particles, which depend on the local shear rate [56].

The most promising model is the one that was originally worked out by Moore [57]. He defined a structural or coherency parameter λ, which is defined to be 1 in a fully saturated state of the structure and to be 0 when all particle bonds are broken. A rate equation for the structural parameter is set up to

consider the creation and the destruction of bonds. It is frequently assumed that all parameters of the Herschel-Bulkley equation are depending on λ [58].

A more detailed model has been set up by Petera et al. [59]. The SSM is modelled as a two-phase system with a semi-fluid approach for the solid phase. A kinetical equation is introduced reflecting the change in structure. The model has been successfully applied for the simulation of die-filling experiments where the flow front was videotaped. Good agreement was achieved between simulation and experiment for the development of the flow front, the transient pressure drop in the die and the final distribution in the solid phase due to segregation [60].

The Cross model considers that at extreme boundary condition, i.e., at very low or very high shear rate, thixotropic fluids assume a Newtonian viscosity [61]. This is expressed by the following equation:

$$\eta = \eta_\infty + \frac{\eta_0 - \eta_\infty}{1 + k\,\dot{\gamma}^n} \tag{4}$$

with η_0 the viscosity for zero shear rate and η_∞ the viscosity for high shear rates and k and n parameters as in the Ostwald de Waele equation.

This model has been applied to fit the experimental results from various researches on SnPb15 alloy in a satisfactory way [62], even though consistent data about the extreme conditions are hardly available in literature and, therefore, the reliability of the model cannot be stated [7]. From the practical point of view, it does not provide an advantage compared with Ostwald de Waele model since the Cross model reduces to the Ostwald de Waele one if the extreme condition viscosities are not determined.

The above-mentioned approaches are applicable if the solid fraction is below approximately 0.65, which corresponds to the maximum packing of the solid particles. Above this value, the SSM can be treated as a "porous solid body" and the approaches of the continuum mechanics must be applied to model the relation between stress and deformation.

5. Steady State Condition: Time-Independent Properties

As aforementioned, it is fundamental to distinguish between the properties of SSM in steady state and transient conditions. In this paragraph, the main findings related to time-independent behavior will be reviewed according to the experimental procedure applied.

Comparison of data available in the literature have been done in the past for A356 and A357 [44]. It was found that the flow curves for both alloys, expressed using a power law relationship, were characterized by a slope of approximately -1, corresponding to the shear exponent. The comparison was carried out among results obtained by means of various techniques and conditions (Figure 8), which is expected to lead to discrepancies in the flow curves, even when studying the same alloy.

As additional evidence of this, Lashkari et al. [63] and Blanco et al. [49] studied a similar Al alloy containing approximately 4.5% Cu using respectively compression tests and shear rate jump experiments with a Searle rheometer. In this case, the difference is also in the range of shear rate investigated since compression tests results correspond to very low shear rates (in the order of 10^{-3}–10^{-2} s^{-1}), while in the other study a very different range was investigated (60–260 s^{-1}).

Regarding shear experiments, more recently Das et al. [64] performed various experiments on A356 alloy with a Searle-type rheometer applying the power law model to evaluate their results. Furthermore, they compared the obtained m and n parameters with the findings of previous researches. The difference between the values was mainly due to the different ranges of shear rates considered for the fitting of the flow curve since Das et al. [64] performed rheological measurements up to 1500 s^{-1} as shear rate values, while the other authors considered a narrower range (approximately up to 200 s^{-1}).

To update the available information, in the present review the attention was focused on the studies from 2003 up to now. Values of flow index and shear exponent for Al alloys were collected from various scientific publications, when available, and they are shown in Tables 1 and 2. It was chosen to organize the data according to the experimental methods used, i.e., shear (Table 1) or compression experiments (Table 2) in order to better represent the rheological behavior of these materials. At this regard, it is

important to mention that experiments with rotational rheometers are useful for the investigation of the rheological behavior of semi-solid slurry with a solid fraction of 0.2–0.5, while compression experiments can provide information for materials characterized by a solid fraction higher than 0.5.

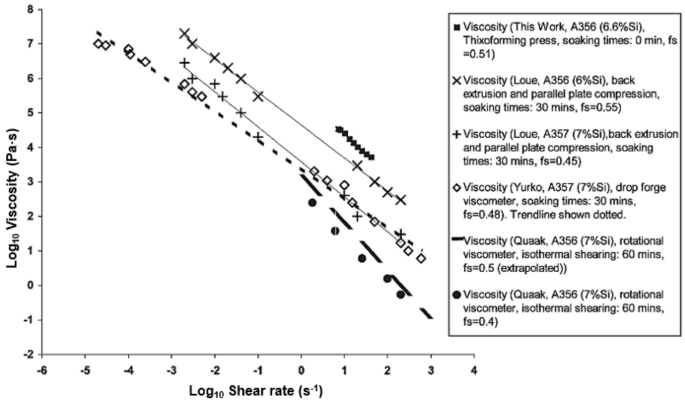

Figure 8. Comparison of apparent viscosities obtained by various experimental techniques and conditions [44].

It appears that the shear exponent assumes values between −1.5 and −1.2 for shear rates up to 300 s^{-1}, while it decreases if a wider shear rate range is applied. Values very close to 0 are found for investigations carried out at low solid fraction. This is reasonable if it is considered that liquid metals exhibit Newtonian behavior. Consequently, it is expected that the flow of semi-solid slurries at low solid fraction would shift towards a Newtonian-like behavior.

Table 1. Power law parameters from experiments with rheometer for different alloys.

	Alloy	Solid Fraction (-)	Shear Rate Range (s^{-1})	Flow Index m (Pa·s^n)	Shear Exponent $n-1$ (-)	Source
1	A356	0.33	3.1–124.8	269	−1.3	[65]
2	AlSi4	0.36	3.1–124.8	325	−1.3	[65]
3	A356	0.2	0–1500	166	−0.92	[64]
4	A356	0.41	0–1500	509	−1.05	[64]
5	A356	0.5	0–1500	589	−1.05	[64]
6	A356	0.4	10–300	789	−1.23	[66]
7	AlSi3	0.4	10–300	122	−1.23	[66]
-	A201 (AlCu4.5)	0.35	60–260	-	−1.35	[49]
-	A201 (AlCu4.5)	0.45	60–260	-	−1.49	[49]
8	AlSi22	0.09	10–50	2.53	−0.34	[50]
9	AlSi30	0.15	10–50	4.63	−0.39	[50]
10	AlSi30	0.20	10–50	109	−1.04	[50]

This is particularly evident if the flow curves corresponding to the parameters listed in Table 1 are plotted in a viscosity vs shear rate graph, as in Figure 9. It clearly appears that the slope of the flow curves obtained for solid fraction above 0.3 are comparable, while for lower values of solid fraction the viscosity is less dependent on the shear rate, reflecting the increasing contribution of the Newtonian liquid phase. Furthermore, also the influence of solid fraction is visible if the results for the same A356 alloys are considered. On the other hand, a scattering in the viscosity values of semi-solid AlSi alloys is observed, which underlines how these kinds of measurements can be affected by various parameters, as such as material preparation, holding time, shear history of the samples, etc. Despite the large number of experiments available in scientific literature, it is still difficult to define viscosity values for SSM in an unambiguous and systematic way.

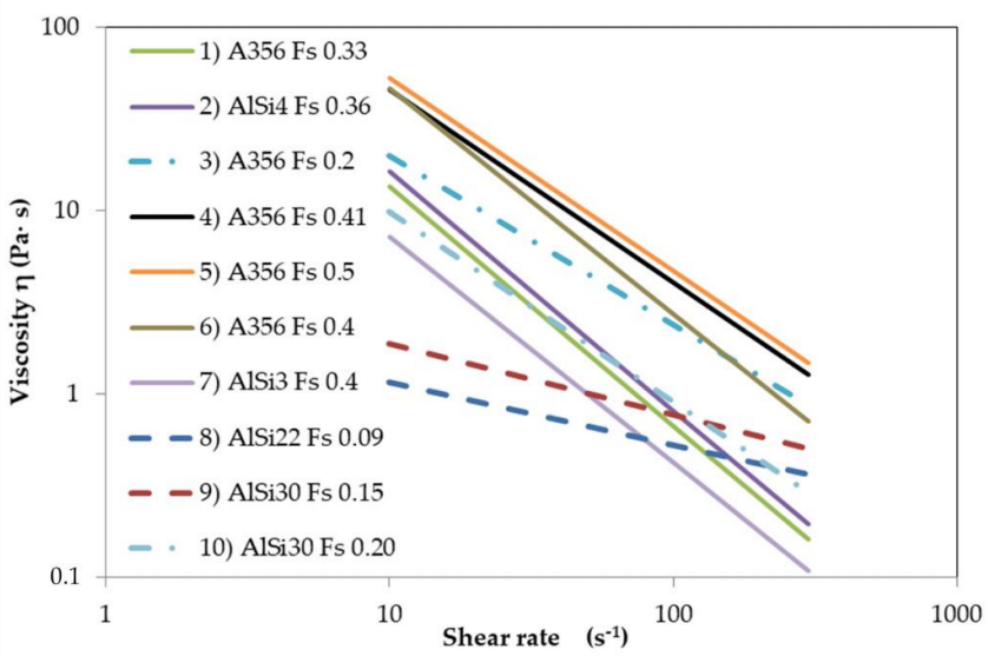

Figure 9. Comparison of flow curves according to parameters reported in the previous Table 1.

It is more complex to perform the same analysis for flow curves obtained from compression experiments, since less abundant data are available in scientific literature, as shown in Table 2.

Table 2. Power law parameters from compression experiments for different alloys.

Alloy	Solid Fraction (-)	Shear Rate Range (s^{-1})	Flow Index m (Pa·s^n)	Shear Exponent $n-1$ (-)	Source
6061	0.5–0.9	0.01–2	10^4–10^6	From −2 to −1 according to the solid fraction	[47]
7075	0.5–0.9	0.01–2	10^4–10^5	approx. −2.5	[47]
2024	0.5–0.9	0.01–2	10^3–10^5	From −2.75 to −2.5 according to the solid fraction	[47]
AlSi25	Various T (°C)	10–3000	1.78×10^7	−1.5	[67]

It is important to mention that most of the shear exponents are negative values. As mentioned above, this gives strange physical results. It must be assumed that the experiments were dominated by secondary effects that influence the experimental results, e.g., wall slippage. The application of these results seems to be doubtful. This is even more evident for the results of the compression tests, which indicate the difficulty to extract reasonable results for the shear behavior from compression tests.

On the other hand, compression experiments can provide important information about the transient and time-dependent properties of SSM close to practical application [68] even when their use for simulation might be doubtful.

6. Non-Viscous Properties

6.1. Yield Stress

It is obvious from the previous explanations that the rheological properties of SSM strongly depend on time—which is frequently forgotten. This is insofar important as any die-filling process, either casting or forging, is a non-stationary process by nature with temporally changing border conditions for the deformation of the material.

An important question is how the typical time scales of the process and the material behavior compare when discussing an appropriate approach to model the material behavior properly [51,69].

This matter becomes evident when investigating the phenomenon of yield stress in SSM. The existence of yield stress is subject of basic discussions, which seem to have philosophical character [70,71]. There is no doubt that the experimental detection of yield stress depends on the quality of the experiment. However, this holds for any mechanical property as well. To identify e.g., thixotropic properties it is necessary to have an instrument with a certain minimal temporal resolution.

In general, it is accepted that the introduction of yield stress for materials with viscoplastic behavior is at least a reasonable engineering approach to model adequately the flow behavior [11,52,72]. As with other materials, the yield stress in SSM is the consequence of the formation of a network of the particles, which is more or less mechanically stable. The direct way to investigate yield stress phenomena is the application of stress or strain ramps and the observation of the temporal behavior of strain or stress respectively [69]. Experiments [6,15] show that the yield stress depends on the solid fraction, the particle size and shape and on the resting time. With increasing resting time, the yield stress increases nearly exponentially, which leads to the concept of three different values of yield stress [15,16]:

- the static one is a constant value and it is achieved after long resting time,
- the dynamic yield stress holds for the period where the yield stress increases with time when the material is in rest after being sheared and
- the isostructural one corresponding to the value which would be measured immediately after shearing the material.

The isostructural value cannot be measured directly and must be found, for instance, by extrapolating the dynamic yield stress to resting zero time. For two Al alloys, it was found that the isostructural yield stress is less than 1/10 of the static value, which was for both alloys about 400 Pa. Comparable experiments have been performed by Solek [73] with high carbon steel, which confirms the above-mentioned findings.

Application of oscillatory shearing and comparison of the temporal development during rest of the yield stress and the loss- and storage-moduli show that the ratio of the both moduli decreases while the yield stress increases [74]. Due to the formation of a stable structure in the material the rheological nature of the material changes from viscous to elastic—fluid to solid—as indicated by the loss angle. The temporal increase of the storage modulus compares with the increase of the yield stress.

The other way to determine yield stress is an indirect one by evaluating the flow curve on the base of an appropriate visco-plastic model. A Herschel-Bulkley model was found to fit in a proper way the experimental results for semi-solid Sn-Pb15 alloy at different solid fractions [60]. The alloy was considered as a homogeneous material with thixotropic properties and it was tested under isothermal conditions. Among the parameters obtained from the application of the model to experimental results, it was possible to calculate finite values of yield stress as a function of the solid fraction. A Herschel–Bulkley approach was applied to the numerical simulation of die filling and it was validated with the results from die-filling experiments [75] using a Sn-Pb alloy. In these experiments, the evolution of the flow front as well as the pressure drop were observed during the die filling and the process was performed for different flow conditions. Similarly, a model corresponding to the Herschel-Bulkley was developed to represent the behavior of semi-solid metallic suspensions in fast transient conditions [76]. The validation of the model was carried out with short time measurements of Sn-Pb15 alloy under rapid shear rate changes, already published by other authors [77]. The model can show the increase of the shear rate in a shear rate jump and the gradual decrease after reaching a maximum. For the yield stress, the authors found interestingly a constant value of 100 Pa, independent of the time the material was in rest (which was between 0 and 5 h).

The evaluation of yield behavior of Al-Si alloys was carried out also using different experimental procedures, as such as the compression and the cone penetration method [72]. Yield stress was measured as a function of temperature, i.e., solid fraction, taking also into account different billet

processing methods, as such as the addition of grain refiner and the application of magneto-hydrodynamic stirring (Figure 10).

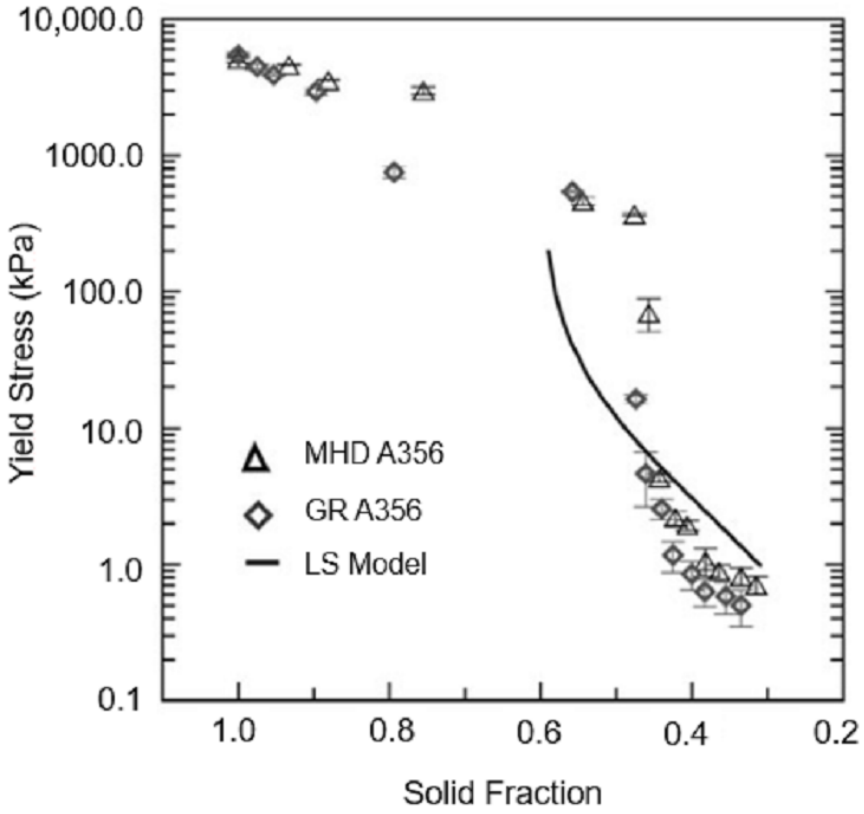

Figure 10. A comparison between measured average yield stresses of grain refined (GR) A356 and magneto-hydrodynamically stirred (MHD) A356 alloys with yield stress values predicted by the Loue–Sigworth (LS) model [72].

It was found that not only the solid fraction is affecting the yield behavior, but that also the entrapped liquid and the morphology of the solid globules can play an important role in determining the deformation resistance. A high amount of entrapped liquid can lead to an increase in yield stress because the "effective" liquid fraction is decreased, while the presence of more rounded solid particles can result in a smaller deformation resistance and, consequently, in a decrease in yield stress.

The viscoplastic behavior of A356 alloy in semi-solid state was expressed by the Herschel-Bulkley model by Simlandi et al. [78]. They also considered a time-dependent structural parameter to comprehensively describe the material behavior at different solid fractions.

An enhanced model based on the Herschel-Bulkley equation was proposed also for other metallic alloys, as such as steels [79] and Mg alloys [80]. Pouyafar et al. [79] calculated the yield stress of M2 steel from the flow curve obtained from experiments in steady-state flow by interpolation of the experimental results to evaluate the stress at zero shear rate. The enhanced model was compared to the classical one and it was found that the new model could predict in a more precise way the behavior of the material, especially at high shear rate, than the conventional one. This was confirmed also by the application of the model to the simulation of the rheometer flow. Moreover, the same model was used to simulate the material behavior during compression test [36].

6.2. Transient Behavior: Time-Dependent Properties

In the introduction, the main thixotropic properties of SSM were briefly discussed. It was mentioned that thixotropic materials show a decrease of viscosity under constant stress and a recovery

of the viscosity when the loading stops. This behavior is linked to microstructural evolution of SSM, in particular to the agglomeration and deagglomeration phenomena.

Various experiments can be performed to better investigate these time-dependent properties, which focus on the response of the SSM to changes in the applied deformation rate or shear stress, as such as shear rate jump or hysteresis loop experiments [60,65,68] or rapid compression tests [45,81].

Modigell et al. [60] investigated thixotropic behavior under isothermal condition on a Sn-Pb15 alloy. Hysteresis loops experiments are particularly useful to provide qualitative information on the degree of thixotropy of the material. It was found that the faster the ramp is performed, the higher the hysteresis area and, therefore, the more evident the thixotropic behavior (Figure 11). On the other hand, Brabazon et al. [65] tested an AlSi4 alloy in a similar way but found that with slower ramp the peak viscosity increases corresponding to an increase in thixotropy, not considering the change around the hysteresis loop. They also evaluated the effect of rest time on the material thixotropy and measured an increase in the viscosity with increasing rest time.

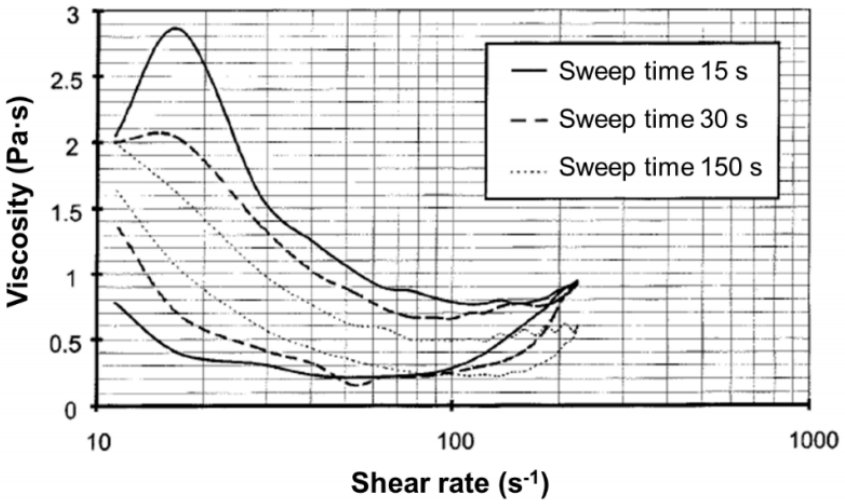

Figure 11. Hysteresis experiments at different sweep times (T = 198 °C, Fs = 0.45) [60].

It is reported [60] that, immediately after an increase in shear rate, the measured viscosity makes a sudden jump and, subsequently, a decrease follows according to the thixotropic nature of the material. The opposite happens when the shear rate is decreased. This phenomenon is said to be "isostructure behavior". It is assumed that the structure of the alloy—corresponding to the initial shear rate—will not change instantaneously to the structure corresponding to the new shear rate. Evaluation of special shear rate jump experiments in terms of an "isostructural flow curve" shows that the SSM immediately after a shear rate jump reacts in a shear thickening way [17]. Recent analyses of the literature [10] regarding this effect confirm the findings of [60]. They showed that it needs a solid fraction larger than 0.36 to be observed. It has been clarified that for shear rate jumps from shear rate zero (sample at rest) this shear thickening effect is masked by yield stress effects.

As above-mentioned, it is important to compare the time scale of the time-dependent rheological properties and the typical process times. Typical process times for die casting or forging are in the order of 1/10 s [40,82], as also confirmed by other authors [83,84] for the thixoforging of steel components. This is interestingly in the order of the response time of modern rotational rheometer. Detailed investigations about kinetics of the thixotropy in SSM are rare. The first well-known investigations of this phenomenon were done by Quaak and Peng et al. [85,86]. Quaak assumed that the process of deagglomeration and agglomeration after a change in shear rate is composed of two steps: a fast process to destroy or create agglomerates and a slow one of coarsening and sintering. This has been confirmed for Sn-Pb alloy by Koke [18], who could model the transient process assuming two different

kinetics. The time scale for the fast process was in the order of 0.5 s—and seemed to be independent of shear rate—whereas the scale of the slow process was 100 times slower. Liu at al. [77] studied the effect of shear jumps on the temporal development of the shear stress for Sn-Pb15 as well (Figure 12). They only investigated the short-term behavior and the time scale they found for the thixotropic effects is comparable with the results of Quaak [85] and Koke.

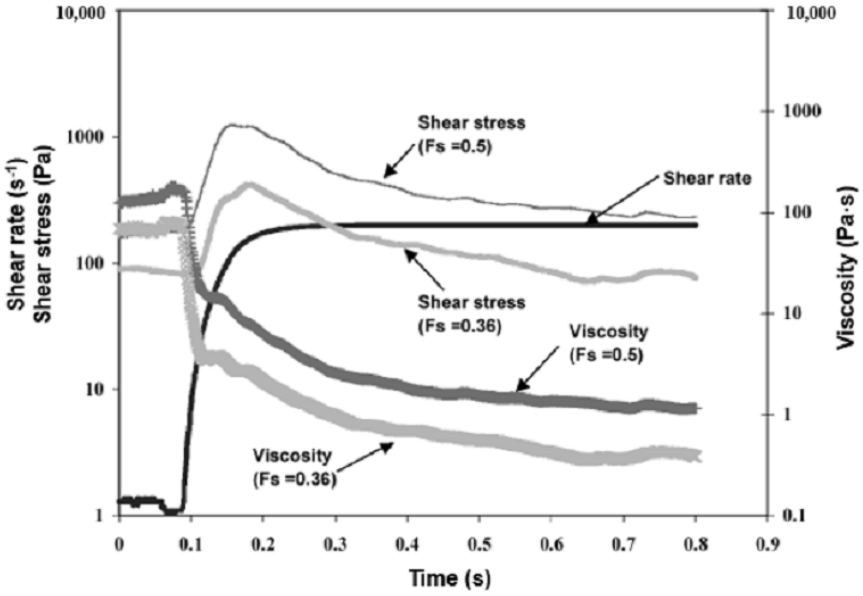

Figure 12. Shear rate jumps (1–200 s^{-1}) for Sn15Pb alloy for two different solid fractions (*Fs* = 0.5 and 0.36) in isothermal condition [77].

Rapid compression tests on AlSi alloys have been performed by Hogg et al. [45], to investigate the rheological properties under the conditions of the real manufacturing process. Time scale of the test has been around 0.065 s, so much shorter than the scale of rotational rheometer. The experiments provided data also about the effect of the holding time and the reheating temperatures. The viscosity estimated from their experiments were by around a factor of ten higher then viscosity values evaluated from shear experiments. Assuming a time scale for the thixotropy of some 1/10 s it can be concluded that in these experiments the material was not in the final state of equilibrium. Based on these studies, also numerical models were developed to describe accurately the transient behavior [30,40,46,76].

Another interesting result regarding thixotropy can be extracted from the work of Bührig-Polaczek et al. [87] who performed experiments with Al 356 with a capillary rheometer. The device, which was developed in house, was equipped with four pressure sensors along the capillary. This allowed evaluating the pressure drop along the path of flow and, consequently, it was possible to analyze the thixotropic reaction of the material. The shear rates they could realize in the capillary were up to 3200 s^{-1} and the resident time in the capillary was in the range of 1/10 s, which compares to typical process times in casting. They found shear thinning behavior in the shear rate range from 1000 to 3200 s^{-1}, whereby the viscosity for 1000 s^{-1} was approximately ten times higher than the viscosity measured in a rotational rheometer at shear rate equal to 250 s^{-1}, which compares with the findings of Hogg [45]. Evaluation of the pressure drop along the capillary showed that the viscosity close to the entrance was around 2.5 Pa·s, while it dropped towards the end of the capillary to 0.6 Pa·s (both for a shear rate of 3200 s^{-1}). The drop was almost linear and showed no tendency to become constant. This indicates that, within the residence time of 0.15 s, the thixotropic reaction is not finalized.

The consequences of this are that obviously the short term and transient behavior of the SSM is of much more interest for the typical casting and forging processes than the equilibrium flow curves.

This is in accordance with numerical analyses of the flow of a viscoplastic material in the gap of a rheometer under conditions relevant for technical processes performed by Alexandrou et al. [30]. They composed the stress function by two contributions: the "steady state" stress, evaluated from long shearing time experiments and assumed to follow a Herschel-Bulkley model, and the stress due to slurry strength, which depends on a coherency parameter, depending on time. The simulation showed that for short times the latter contribution is dominant and defines the propagation of the shear in the gap. The relevant time frame is in the order of less than 0.1 s. Evaluation of experiments in this time scale need the application of computational rheology rather than the classical evaluation of the experimental data.

7. Ostwald Ripening

Another important aspect to consider to completely describe the rheological behavior of SSM is the growth and coarsening of the globular solid particles under rest or shear condition by recrystallization. This will happen under isothermal conditions. The phenomenon is usually indicated as Ostwald ripening and it takes place in different materials, as such as emulsion systems, etc. During this process, small particles dissolve, while the larger ones coarsen with the consequence that the surface energy is minimized [88] so that in total the mean particle diameter in the material will increase.

This phenomenon was investigated in the past by several researches [89–92] mainly by means of the observation of 2D sections of samples quenched from the semi-solid state, which represented a serious limitation in the investigation of the real phenomenon. More recently, agglomeration and growth of necks between solid particles, which are different from Ostwald ripening, and the later were investigated by X-ray in situ tomography [93,94].

In systems in rest, Ostwald ripening is a diffusion-controlled process that is rather slow and has less technical importance in the frame of the subjects discussed here. The growth of the particle as a function of time can be calculated on the base of the LSW-theory (Lifshitz, Sloyozov [95] and Wagner [96]) which gives a linear relationship between the volume of the particle and the time. In agitated systems, the growth of the particle is strongly enhanced by convective transport, which results in a growth of particles in a time frame which is at least relevant for a couple of experimental investigations.

The rheological effect of the Ostwald ripening is a decrease of the viscosity because of the increase of the mean particle diameter in the sample—although solid fraction will not change because of isothermal condition. This effect is demonstrated in Figure 13.

The Sn-Pb melt, initially fully liquid, is cooled down into the two-phase condition. First, the viscosity will rise, subsequently it will reach a maximum and will start to drop. The first decrease after the maximum is due to the formation of non-dendritic particles. At the first small peak, this process is more or less finalized. The further decrease of the viscosity is mainly due to convective Ostwald ripening. The increase in particle size is clearly demonstrated in the metallographic pictures. The time scale of this process is in the order of 60 min, depending on the shear rate. The higher the shear rate, the faster the growth.

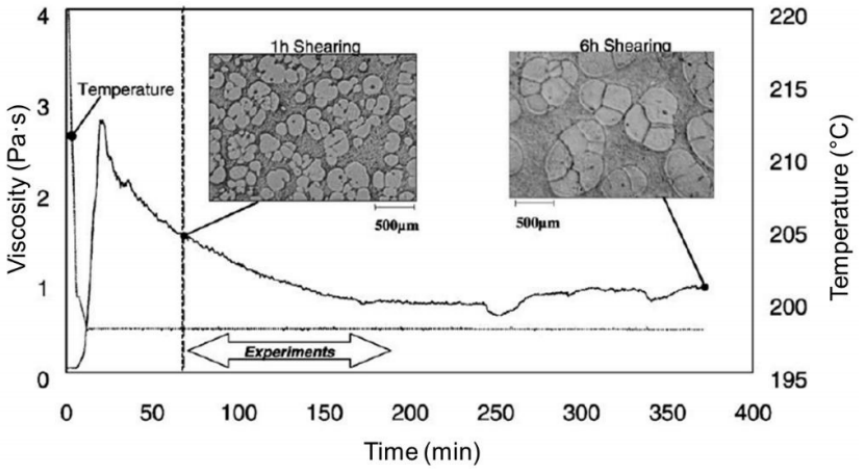

Figure 13. Viscosity vs. time at constant shear rate (110 s^{-1}). Initial cooling rate is 1 °C/min. Steady-state temperature is 198 °C, corresponding to a solid fraction *Fs* = 0.45. The metallographic pictures show samples quenched after 1 and 6 h of constant shearing (Sn–15% Pb) [17].

It is obvious that the Ostwald ripening falsifies the experimental results when performing long-term investigations, such as, for example, making shear rate jump experiments. For instance, in the case of A356 alloy tested in a rotational rheometer at 0.40 solid fraction, it can be seen in Figure 14 that at the end of the experiment the viscosity for a shear rate of 80 s^{-1} is significantly lower than at the beginning. Evaluation of these data will result in an overestimation of the shear thinning effect. Modigell et al. [97] have developed a simple model considering convective transport in the system, which allows correcting the data for any shear, as shown in Figure 14. For sufficient large shear rates, the temporal change of the diameter is linear with time.

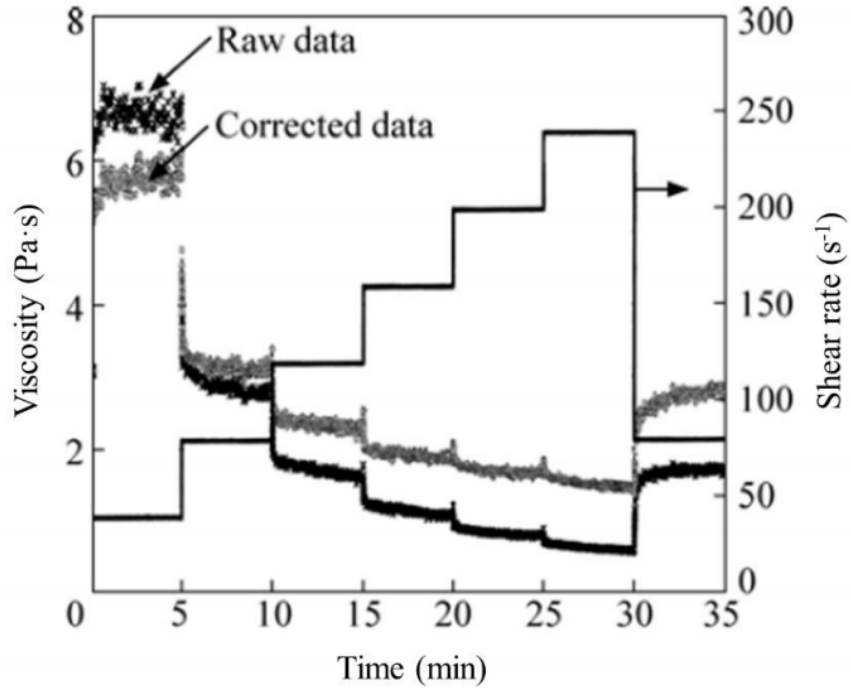

Figure 14. Shear rate experiment results with A356 under solid fraction of 0.40 [97].

The effect of isothermal and non-isothermal stirring on particle size was also evaluated for Al-Si alloys [98–101] and Mg alloys [102]. Sukumaran et al. [99] investigated the evolution of particle

diameter with shearing time for an Al-Si alloy with and without the addition of grain refiner (Figure 15). In this case, it was found that first the particle size decreases due to the fragmentation of the dendritic structure. Subsequently, particle size reaches a minimum value before starting to increase due to the discussed Ostwald ripening mechanism, which is considered the main mechanism for coarsening of solid globules, while agglomeration phenomena is believed to contribute in a minor way. Due to the presence of the grain refiner, the growth of dendrites during semi-solid processing is inhibited, promoting the formation of an equiaxed microstructure, in comparison with the base material, and accelerating the formation of a globular microstructure, as well as the coarsening and ripening phenomena. Therefore, the coarsening of particles takes place earlier for the alloy with grain refiner in comparison with the base alloy, as visible in Figure 15.

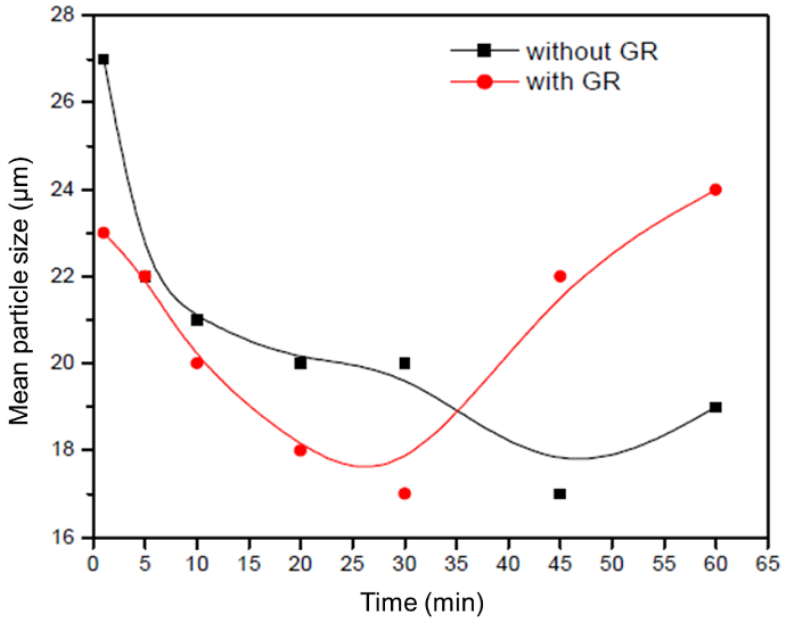

Figure 15. Plot of nominal particle diameter vs. time of isothermal stirring (shear rate 210 s^{-1}) at 615 °C [99].

The same mechanism is illustrated also by Chen et al. [102], who provided the following schematic diagram (Figure 16) and correlated the evolution of the particle size to the apparent viscosity for a Mg alloy.

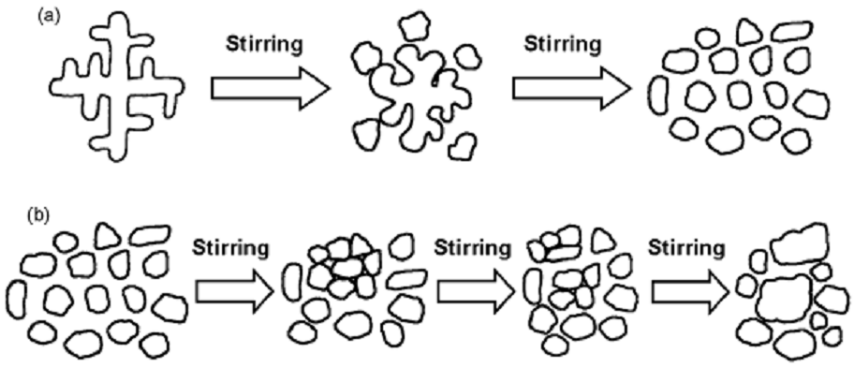

Figure 16. Schematic diagram of the variation of microstructure for: (**a**) decreasing apparent viscosity and (**b**) increasing apparent viscosity [102].

8. Summary

In the present review, a summary of the basic aspects of the rheology of semi-solid metals are presented. These materials exhibit a complex behavior and several parameters must be considered to correctly characterize it. For this reason, the distinction between steady state and time-dependent properties is fundamental. Furthermore, additional important aspects as the evaluation of yield stress and Ostwald ripening mechanism are discussed.

In general, the analyses of the recent literature show that a lot of experimental and theoretical work has been done and that the initial findings of the early researches are confirmed. A database has been provided for higher melting alloys due to technical development in the field of rheometers. Even for steels, basic data are now available provided by shear experiments.

Most of the data give information about rheological behavior under equilibrium conditions. In technical practice, the processes are far from equilibrium due to the high process speeds. For better understanding of the process phenomena and for reliable simulation of the forming process, the short-term behavior of the SSM must be investigated more deeply than it has been done up to now. This means that the thixotropic properties, as well as the yield phenomena, must be studied to clearly understand the process phenomena under technical conditions. Additionally, there is a lack of knowledge in the relationship between the composition of the alloy and the rheological properties.

Conflicts of Interest: The authors declare no conflict of interest.

References

1. Flemings, M.C. Behavior of metal alloys in the semisolid state. *Metall. Trans. A* **1991**, *22*, 957–981. [CrossRef]
2. Hirt, G.; Kopp, R. *Thixoforming: Semi-Solid Metal Processing*; Wiley-VCH Verlag GmbH & Co. KGaA: Weinheim, Germany, 2009.
3. Pola, A.; Montesano, L.; Tocci, M.; La Vecchia, G.M. Influence of Ultrasound Treatment on Cavitation Erosion Resistance of AlSi7 Alloy. *Materials* **2017**, *10*, 256. [CrossRef] [PubMed]
4. Barnes, H.A.; Hutton, J.F.; Walters, K. *An Introduction to Rheology*; Elsevier Science: Amsterdam, The Netherlands, 1993.
5. Bakhtiyarov, S.I.; Overfelt, R.A. Measurement of liquid metal viscosity by rotational technique. *Acta Mater.* **1999**, *47*, 4311–4319. [CrossRef]
6. Modigell, M.; Koke, J. Rheological modelling on semi-solid metal alloys and simulation of thixocasting processes. *J. Mater. Process. Tech.* **2001**, *111*, 53–58. [CrossRef]
7. Atkinson, H.V. Modelling the semisolid processing of metallic alloys. *Prog. Mater. Sci.* **2005**, *50*, 341–412. [CrossRef]
8. Atkinson, H.; Favier, V. Does Shear Thickening Occur in Semisolid Metals? *Metall. Mater. Trans. A* **2016**, *47*, 1740–1750. [CrossRef]
9. Lashkari, O.; Ghomashchi, R. The implication of rheology in semi-solid metal processes: An overview. *J. Mater. Process. Tech.* **2007**, *182*, 229–240. [CrossRef]
10. Kirkwood, D.H.; Suery, M.; Kapranos, P.; Atkinson, H.V.; Young, K.P. *Semi-Solid Processing of Alloys*; Springer: Berlin, Germany, 2009.
11. McLelland, A.R.A.; Henderson, N.G.; Atkinson, H.V.; Kirkwood, D.H. Anomalous rheological behaviour of semi-solid alloy slurries at low shear rates. *Mater. Sci. Eng. A* **1997**, *232*, 110–118. [CrossRef]
12. Hirt, G.; Uggowitzer, P.J.; Bleck, W.; Friedrich, B.; Schneider, J.M.; Modigell, M.; Kopp, R.; Bobzin, K.; Telle, R.; Bührig-Polaczek, A.; et al. *Final Report of the Joint Research Program SFB289 Forming of Metals in the Semi-Solid State and Their Properties*; RWTH-Aachen University: Aachen, Germany, 2007.
13. Quaak, C.J.; Katgermann, L.; Kool, W.H. Viscosity Evaluation of Partially Solidified Aluminium Slurries after a Shear Rate Jump. In Proceedings of the 4th International Conference on Semi-Solid Processing of Alloys and Composites, Sheffield, UK, 19–21 June 1996.
14. Windhab, E.J. Process–Structure–Rheology Relationships of Multiphase Food Systems. In Proceedings of the 1st International Symposium on Food Rheology and Structure, Zurich, Switzerland, 16–21 March 1997.

15. Modigell, M.; Hufschmidt, M. Dynamic and Static Yield Stress of Metallic Suspensions. *Solid State Phenom.* **2006**, *116–117*, 587–590. [CrossRef]
16. Moll, A.; Modigell, M. Yield stress phenomena in semi-solid alloys. *Int. J. Mater. Form.* **2010**, *3*, 779–782. [CrossRef]
17. Koke, J.; Modigell, M. Flow behaviour of semi-solid metal alloys. *J. Non-Newton. Fluid. Mech.* **2003**, *112*, 141–160. [CrossRef]
18. Koke, J. *Rheologie Teilerstarrter Metalllegierungen*; Fortschr.-Ber. VDI Reihe 5 Nr. 620; VDI Verlag: Düsseldorf, Germany, 2001; Volume 620.
19. Harboe, S.J. *Investigation of Rheological and Microstructural Properties of Semi-Solid Aluminium Copper Alloy during Isothermal Shear*; Shaker Verlag GmbH: Aachen, Germany, 2017.
20. Zabler, S.; Rueda, A.; Rack, A.; Riesemeier, H.; Zaslansky, P.; Manke, I.; Garcia-Moreno, F.; Benhart, J. Coarsening of grain-refined semi-solid Al-Ge32 alloy: X-ray microtomography and in situ radiography. *Acta Mater.* **2007**, *55*, 5045–5055. [CrossRef]
21. Cai, B.; Karagadde, S.; Rowley, D.; Marrow, T.J.; Connolley, T.; Lee, P.D. Time-resolved synchrotron tomographic quantification of deformation-induced flow in a semi-solid equiaxed dendritic Al-Cu alloy. *Scr. Mater.* **2015**, *103*, 69–72. [CrossRef]
22. Kareh, K.M.; Lee, P.D.; Atwood, R.C.; Connolley, T.; Gourlay, C.M. Revealing the micromechanisms behind semi-solid metal deformation with time-resolved X-ray tomography. *Nat. Commun.* **2014**, *5*, 1–7. [CrossRef] [PubMed]
23. Terzi, S.; Salvo, L.; Suery, M.; Dahle, A.; Boller, E. In situ microtomography investigation of microstructural evolution in Al-Cu alloys during holding in semi-solid state. *Trans. Nonferr. Metals Soc. China* **2010**, *20*, s734–s738. [CrossRef]
24. Modigell, M.; Pola, A.; Suery, M.; Zang, C. Investigation of correlations between shear history and microstructure of semi-solid alloys. *Solid State Phenom.* **2013**, *192–193*, 251–256. [CrossRef]
25. Kang, C.G.; Choi, J.S.; Kim, K.H. The effect of strain rate on macroscopic behavior in the compression forming of semi-solid aluminum alloy. *J. Mater. Process. Tech.* **1999**, *88*, 159–168. [CrossRef]
26. Macosko, C.W. *Rheology—Principles, Measurements, and Applications*; Wiley-VCH, Inc.: Hoboken, NJ, USA, 1994.
27. Van Wazer, J.R.; Lyons, J.; Lim, K.; Colwell, R.E. *Viscosity and Flow Measurements*; Wiley: New York, NY, USA, 1963.
28. Schummer, P.; Worthoff, R.H. An elementary method for the evaluation of a flow curve. *Chem. Eng. Sci.* **1978**, *33*, 759–763. [CrossRef]
29. Alexandrou, A.N.; Georgiou, G.C.; Economides, E.-A.; Modigell, M. Determining true material constants of semisolid slurries from rotational rheometer data. *Solid State Phenom.* **2016**, *256*, 153–172. [CrossRef]
30. Alexandrou, A.N.; Georgiou, G. On the early breakdown of semisolid suspensions. *J. Non-Newton. Fluid Mech.* **2007**, *142*, 199–206. [CrossRef]
31. Modigell, M.; Pape, L. A comparison of measuring devices used to prevent wall slip in viscosity measurements of metallic suspensions. *Solid State Phenom.* **2008**, *141–143*, 307–312. [CrossRef]
32. Kiljański, T. A method for correction of the wall-slip effect in a Couette rheometer. *Rheol. Acta* **1989**, *28*, 61–64. [CrossRef]
33. Harboe, S.; Modigell, M. Wall slip of semi-solid A356 in couette rheometers. *AIP Conf. Proc.* **2011**, *1353*, 1075–1080. [CrossRef]
34. Tocci, M.; Zang, C.; Cadórniga Zueco, I.; Pola, A.; Modigell, M. Rheological properties of liquid metals and semisolid materials at low solid fraction. *Solid State Phenom.* **2016**, *256*, 133–138. [CrossRef]
35. Solek, K.; Rogal, L.; Kapranos, P.; Solek, K.P.; Rogal, L.; Kapranos, P. Evolution of Globular Microstructure and Rheological Properties of Stellite 21 Alloy after Heating to Semisolid State. *J. Mater. Eng. Perform.* **2017**, *26*, 115–122. [CrossRef]
36. Yekta, F.H.; Vanini, A.S. Simulation the Flow of Semi-Solid Steel Alloy Using an Enhanced Model. *Metals Mater. Int.* **2015**, *21*, 913–922. [CrossRef]
37. Modigell, M.; Volkmann, T.; Zang, C. A High -Precision Rotational Rheometer for Temperatures up to 1700 °C. *Solid State Phenom.* **2013**, *192–193*, 359–364. [CrossRef]
38. Laxmanan, V.; Flemings, M.C. Deformation of Semi-Solid Sn-15 Pct Pb Alloy. *Metall. Trans. A* **1980**, *11*, 1927–1937. [CrossRef]
39. Nafisi, S.; Lashkari, O.; Ghomashchi, R.; Ajersch, F.; Charette, A. Microstructure and rheological behavior of grain refined and modified semi-solid A356 Al–Si slurries. *Acta Mater.* **2006**, *54*, 3503–3511. [CrossRef]

40. Hu, X.G.; Zhu, Q.; Atkinson, H.V.; Lu, H.X.; Zhang, F.; Dong, H.B.; Kang, Y.L. A time-dependent power law viscosity model and its application in modelling semi-solid die casting of 319s alloy. *Acta Mater.* **2017**, *124*, 410–420. [CrossRef]
41. Becker, E.; Favier, V.; Bigot, R.; Cezard, P.; Langlois, L. Impact of experimental conditions on material response during forming of steel in semi-solid state. *J. Mater. Process. Tech.* **2010**, *210*, 1482–1492. [CrossRef]
42. Becker, E.; Langlois, L.; Favier, V.; Bigot, R. Thermomechanical modelling and simulation of C38 thixoextrusion steel. *Solid State Phenom.* **2015**, *217–218*, 130–137. [CrossRef]
43. Shimahara, H.; Baadjou, R.; Kopp, R.; Hirt, G. Investigation of flow behavior and microstructure on X210CrW12 steel in semi-solid state. *Solid State Phenom.* **2006**, *116–117*, 189–192. [CrossRef]
44. Liu, T.Y.; Atkinson, H.V.; Kapranos, P.; Kirkwood, D.H.; Hogg, S.C. Rapid Compression of Aluminum Alloys and Its Relationship to Thixoformability. *Metall. Mater. Trans. A* **2003**, *34*, 1545–1554. [CrossRef]
45. Hogg, S.C.; Atkinson, H.V.; Kapranos, P. Semi-Solid Rapid Compression Testing of Spray-Formed Hypereutectic Al-Si Alloys. *Metall. Mater. Trans. A* **2004**, *35*, 899–910. [CrossRef]
46. Favier, V.; Atkinson, H.V. Micromechanical modelling of the elastic–viscoplastic response of metallic alloys under rapid compression in the semi-solid state. *Acta Mater.* **2011**, *59*, 1271–1280. [CrossRef]
47. Kim, W.Y.; Kang, C.G.; Kim, B.M. The effect of the solid fraction on rheological behavior of wrought aluminum alloys in incremental compression experiments with a closed die. *Mat. Sci. Eng. A* **2007**, *447*, 1–10. [CrossRef]
48. Joly, P.A.; Mehrabian, R. The rheology of a partially solid alloy. *J. Mater. Sci.* **1976**, *11*, 1393–1418. [CrossRef]
49. Blanco, A.; Azpilgain, Z.; Lozares, J.; Kapranos, P.; Hurtado, I. Rheological characterization of A201 aluminum alloy. *Trans. Nonferr. Metals Soc. China* **2010**, *20*, 1638–1642. [CrossRef]
50. Heidary, D.S.B.; Akhlaghi, F. Experimental Investigation on the Rheological Behavior of Hypereutectic Al-Si Alloys by a Precise Rotational Viscometer. *Metall. Mater. Trans. A* **2010**, *41*, 3435–3442. [CrossRef]
51. Chhabra, R.P.; Richardson, J.F. *Non-Newtonian Flow in the Process Industries*; Butterworth Heinemann: Oxford, UK, 2004.
52. Burgos, G.R.; Alexandrou, A.N.; Entov, V. Thixotropic rheology of semisolid metal suspensions. *J. Mater. Process. Tech.* **2001**, *110*, 164–176. [CrossRef]
53. Burgos, G.R.; Alexandrou, A.N. Flow development of Herschel-Bulkley fluids in a sudden three-dimensional square expansion. *J. Rheol.* **1999**, *43*, 485–498. [CrossRef]
54. Ahmed, A.; Alexandrou, A.N. Processing of semi-solid materials using a shear-thickening Bingham fluid model. *Am. Soc. Mech. Eng. Fluids Eng. Div.* **1994**, *179*, 83–87.
55. Barnes, H.A. Thixotropy—A review. *J. Non-Newton. Fluid Mech.* **1997**, *70*, 1–33. [CrossRef]
56. Denny, D.A.; Brodkey, R.S. Kinetic Interpretation of Non-Newtonian Flow. *J. Appl. Phys.* **1962**, *33*, 2269–2274. [CrossRef]
57. Moore, F. The rheology of ceramic slips and bodies. *Trans. Brit. Ceram. Soc.* **1959**, *58*, 470–494.
58. Tonmukayakul, N.; Pan, Q.Y.; Alexandrou, A.N.; Apelian, D. Transient Flow Characteristics and Properties of Semi Solid Aluminium Alloy A356. In Proceedings of the 8th International Conference on Semi-Solid Processing of Alloys and Composites, Limassol, Cyprus, 21–23 September 2004; pp. 167–172.
59. Petera, J.; Kotynia, M. The numerical simulation of the thixoforming. *Inzynieria Chem. Proces.* **2001**, *22*, 1103–1108.
60. Modigell, M.; Koke, J. Time-Dependent Rheological Properties of Semi-Solid Metal Alloys. *Mech. Time-Depend. Mater.* **1999**, *3*, 15–30. [CrossRef]
61. Cross, M.M. Rheology of Non-Newtonian Fluids: A New Flow Equation for Pseudoplastic Systems. *J. Colloidal Sci.* **1965**, *20*, 417–437. [CrossRef]
62. Liu, T.Y. Rheology of Semisolid Alloys under Rapid Change in Shear Rate. Ph.D. Thesis, University of Sheffield, Sheffield, UK, 2002.
63. Lashkari, O.; Ajersch, F.; Charette, A.; Chen, X.-G. Microstructure and rheological behavior of hypereutectic semi-solid Al–Si alloy under low shear rates compression test. *Mater. Sci. Eng. A* **2008**, *492*, 377–382. [CrossRef]
64. Das, P.; Samanta, S.K.; Dutta, P. Rheological Behavior of Al-7Si-0.3Mg Alloy at Mushy State. *Metall. Mater. Trans. B* **2015**, *46*, 1302–1313. [CrossRef]
65. Brabazon, D.; Browne, D.J.; Carr, A.J. Experimental investigation of the transient and steady state rheological behaviour of Al-Si alloys in the mushy state. *Mater. Sci. Eng. A* **2003**, *356*, 69–80. [CrossRef]

66. Tocci, M.; Pola, A.; La Vecchia, G.M.; Modigell, M. Characterization of a New Aluminium Alloy for the Production of Wheels by Hybrid Aluminium Forging. *Procedia Eng.* **2015**, *109*, 303–311. [CrossRef]
67. Fukui, Y.; Nara, D.; Kumazawa, N. Evaluation of the Deformation Behavior of a Semi-solid Hypereutectic Al-Si Alloy Compressed in a Drop-Forge Viscometer. *Metall. Mater. Trans. A* **2015**, *46*, 1908–1916. [CrossRef]
68. Azzi, L.; Ajersch, F. Analytical Modeling of the Rheological Behavior of Semisolid Metals and Composites. *Metall. Mater. Trans. B* **2006**, *37*, 1067–1074. [CrossRef]
69. Cheng, D.C.-H. Yield stress: A time-dependent property and how to measure it. *Rheol. Acta* **1986**, *25*, 542–554. [CrossRef]
70. Barnes, H.A.; Walters, K. The yield stress myth? *Rheol. Acta* **1985**, *24*, 323–326. [CrossRef]
71. Barnes, H.A. The yield stress—A review or 'παντα ρει'—Everything flows? *J. Non-Newton. Fluid Mech.* **1999**, *81*, 133–178. [CrossRef]
72. Pan, Q.Y.; Apelian, D.; Alexandrou, A.N. Yield Behavior of Commercial Al-Si Alloys in the Semisolid State. *Metall. Mater. Trans. B* **2004**, *35*, 1187–1202. [CrossRef]
73. Solek, K. Identification of the steel viscosity and dynamic yield stress for the numerical modelling of casting simulations in the semi-solid state. *Arch. Metall. Mater.* **2017**, *62*, 195–200. [CrossRef]
74. Harboe, S.; Modigell, M. Yield stress in semi-solid alloys—The dependency on time and deformation history. *Key Eng. Mater.* **2013**, *554–557*, 523–535. [CrossRef]
75. Hufschmidt, M.; Modigell, M.; Petera, J. Modelling and simulation of forming processes of metallic suspensions under non-isothermal conditions. *J. Non-Newton. Fluid Mech.* **2006**, *134*, 16–26. [CrossRef]
76. Gautham, B.P.; Kapur, P.C. Rheological model for short duration response of semi-solid metals. *Mater. Sci. Eng. A* **2005**, *393*, 223–228. [CrossRef]
77. Liu, T.Y.; Atkinson, H.V.; Ward, P.J.; Kirkwood, D.H. Response of Semi-solid Sn-15 Pct Pb to Rapid Shear-Rate Changes. *Metall. Mater. Trans. A* **2003**, *34*, 409–417. [CrossRef]
78. Simlandi, S.; Barman, N.; Chattopadhyay, H. Study on Rheological Behavior of Semisolid A356 Alloy during Solidification. *Trans. Indian Inst. Metals* **2012**, *65*, 809–814. [CrossRef]
79. Pouyafar, V.; Sadough, S.A. An Enhanced Herschel–Bulkley Model for Thixotropic Flow Behavior of Semisolid Steel Alloys. *Metall. Mater. Trans. B* **2013**, *44*, 1304–1310. [CrossRef]
80. Liang, L.; Mian, Z. Theoretical research on rheological behavior of semisolid slurry of magnesium alloy AZ91D. *Comput. Mater. Sci.* **2015**, *102*, 202–207. [CrossRef]
81. Omar, M.Z.; Atkinson, H.V.; Kapranos, P. Thixotropy in Semisolid Steel Slurries under Rapid Compression. *Metall. Mater. Trans. A* **2011**, *42*, 2807–2819. [CrossRef]
82. Kirkwood, D.H.; Ward, P.J. Numerical Modelling of Semi-Solid Flow under Processing Conditions. *Fundam. Thixoforming Process.* **2004**, *75*, 519–524. [CrossRef]
83. Becker, E.; Bigot, R.; Rivoirard, S.; Faverolle, P. Experimental investigation of the thixoforging of tubes of low-carbon steel. *J. Mater. Process. Tech.* **2018**, *252*, 485–497. [CrossRef]
84. Lozares, J.; Azpilgain, Z.; Hurtado, I.; Ortubay, R.; Berrocal, S. Thixo Lateral Forging of a Commercial Automotive Spindle From LTT45 Steel Grade. *Key Eng. Mater.* **2012**, *504–506*, 357–360. [CrossRef]
85. Quaak, C.J. Rheology of Partially Solidified Aluminium Alloys and Composites. Ph.D. Thesis, Technische Univesiteit Delft, Delft, The Netherlands, 1996.
86. Peng, H.; Wang, K.K. Steady State and Transient Rheological Behaviour of a Semi-Solid Tin-Lead Alloy in Simple Shear Flow. In Proceedings of the 4th International Conference Semi-Solid Processing of Alloys and Composites, Sheffield, UK, 19–21 June 1996; pp. 2–9.
87. Bührig-Polaczek, A.; Afrath, C.; Modigell, M.; Pape, L. Comparison of rheological measurement techniques for semi-solid aluminium alloys. *Solid State Phenom.* **2006**, *116–117*, 610–613. [CrossRef]
88. Tadros, T. (Ed.) Ostwald Ripening. In *Encyclopedia of Colloid and Interface Science*, 1st ed.; Springer: Berlin/Heidelberg, Germany, 2013.
89. Courtney, T.H. Microstructural evolution during liquid phase sintering: Part II. Microstructural coarsening. *Metall. Trans. A* **1976**, *8*, 685–689. [CrossRef]
90. Courtney, T.H. A reanalysis of the kinetics of neck growth during liquid phase sintering. *Metall. Trans. A* **1977**, *8*, 671–677. [CrossRef]
91. Poirier, D.R.; Ganesan, S.; Andrews, M.; Ocansey, P. Isothermal coarsening of dendritic equiaxial grains in Al–15.6 wt %Cu alloy. *Mater. Sci. Eng. A* **1991**, *148*, 289–297. [CrossRef]

92. Bender, W.; Ratke, L. Ostwald ripening of liquid phase sintered Cu Co dispersions at high volume fractions. *Acta Mater.* **1998**, *46*, 1125–1133. [CrossRef]
93. Limodin, N.; Salvo, L.; Suery, M.; DiMichiel, M. In situ investigation by X-ray tomography of the overall and local microstructural changes occurring during partial remelting of an Al–15.8 wt % Cu alloy. *Acta Mater.* **2007**, *55*, 3177–3191. [CrossRef]
94. Terzi, S.; Salvo, L.; Suery, M.; Dahle, A.K.; Boller, E. Coarsening mechanisms in a dendritic Al–10% Cu alloy. *Acta Mater.* **2010**, *58*, 20–30. [CrossRef]
95. Lifshitz, I.M.; Sloyozov, V.V. The kinetics of precipitation from supersaturated solid solutions. *J. Phys. Chem. Solids* **1961**, *19*, 35–50. [CrossRef]
96. Wagner, C. Theorie der alterung von niederschlägen durch umlösung. *Z. Elektrochem.* **1961**, *65*, 581–591.
97. Modigell, M.; Pola, A. Modeling of shear induced coarsening effects in semi-solid alloys. *Trans. Nonferr. Metals Soc. China* **2010**, *20*, 1696–1701. [CrossRef]
98. Yang, Y.S.; Tsao, C.-Y.A. Viscosity and structure variations of Al–Si alloy in the semi-solid state. *J. Mater. Sci.* **1997**, *32*, 2087–2092. [CrossRef]
99. Sukumaran, K.; Pai, B.C.; Chakraborty, M. The effect of isothermal mechanical stirring on an Al–Si alloy in the semisolid condition. *Mater. Sci. Eng. A* **2004**, *369*, 275–283. [CrossRef]
100. Barman, N.; Dutta, P. Rheology of A356 Alloy during Solidification under Stirring. *Trans. Indian Inst. Metals* **2014**, *67*, 101–104. [CrossRef]
101. Rogal, L.; Dutkiewicz, J.; Atkinson, H.V.; Lityńska-Dobrzyńska, L.; Czeppe, T.; Modigell, M. Characterization of semi-solid processing of aluminium alloy 7075 with Sc and Zr additions. *Mater. Sci. Eng. A* **2013**, *580*, 362–373. [CrossRef]
102. Chen, H.I.; Chen, J.C.; Liao, J.J. The influence of shearing conditions on the rheology of semi-solid magnesium alloy. *Mater. Sci. Eng. A* **2008**, *487*, 114–119. [CrossRef]